

Accepted Manuscript

Electrochemical reactions of catechol, methylcatechol and dopamine at tetrahedral amorphous carbon (ta-C) thin film electrodes

Tommi Palomäki, Sara Chumillas, Sami Sainio, Vera Protopopova, Minna Kauppila, Jari Koskinen, Víctor Climent, Juan M. Feliu, Tomi Laurila

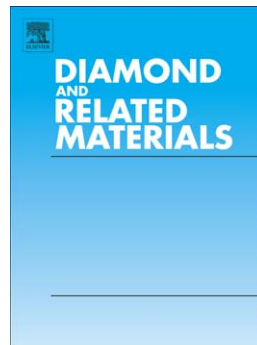
PII: S0925-9635(15)30034-0
DOI: doi: [10.1016/j.diamond.2015.09.003](https://doi.org/10.1016/j.diamond.2015.09.003)
Reference: DIAMAT 6456

To appear in: *Diamond & Related Materials*

Received date: 7 July 2015
Revised date: 3 September 2015
Accepted date: 4 September 2015

Please cite this article as: Tommi Palomäki, Sara Chumillas, Sami Sainio, Vera Protopopova, Minna Kauppila, Jari Koskinen, Víctor Climent, Juan M. Feliu, Tomi Laurila, Electrochemical reactions of catechol, methylcatechol and dopamine at tetrahedral amorphous carbon (ta-C) thin film electrodes, *Diamond & Related Materials* (2015), doi: [10.1016/j.diamond.2015.09.003](https://doi.org/10.1016/j.diamond.2015.09.003)

This is a PDF file of an unedited manuscript that has been accepted for publication. As a service to our customers we are providing this early version of the manuscript. The manuscript will undergo copyediting, typesetting, and review of the resulting proof before it is published in its final form. Please note that during the production process errors may be discovered which could affect the content, and all legal disclaimers that apply to the journal pertain.



Electrochemical Reactions of Catechol, Methylcatechol and Dopamine at Tetrahedral Amorphous Carbon (ta-C) Thin Film Electrodes

Tommi Palomäki^a, Sara Chumillas^b, Sami Sainio^a, Vera Protopopova^c, Minna Kauppila^d, Jari Koskinen^c, Víctor Climent^b, Juan M. Feliu^b and Tomi Laurila^{a*}

^a Department of Electrical Engineering and Automation, School of Electrical Engineering, Aalto University, P.O. Box 13500, 00076 Aalto, Finland

^b Instituto Universitario de Electroquímica, Universidad de Alicante, Apartado 99, E-03080, Alicante, Spain

^c Department of Materials Science and Engineering, School of Chemical Technology, Aalto University, P.O. Box 16200, 00076 Aalto, Finland

^d Department of Applied Physics, School of Science, Aalto University, P.O. Box 11000, 00076 Aalto, Finland

*Corresponding author:

Tel: +358503414375, e-mail: tomi.laurila@aalto.fi

Abstract

The electrochemical reactions of dopamine, catechol and methylcatechol were investigated at tetrahedral amorphous carbon (ta-C) thin film electrodes. In order to better understand the reaction mechanisms of these molecules, cyclic voltammetry with varying scan rates was carried out at different pH values in H₂SO₄ and PBS solutions. The results were compared to the same redox reactions taking place at glassy carbon (GC) electrodes. All three catechols exhibited quasi-reversible behavior with sluggish electron transfer kinetics at the ta-C electrode. At neutral and alkaline pH, rapid coupled homogeneous reactions followed the oxidation of the catechols to the

corresponding o-quinones and led to significant deterioration of the electrode response. At acidic pH, the extent of deterioration was considerably lower. All the redox reactions showed significantly faster electron transfer kinetics at the GC electrode and it was less susceptible toward surface passivation. An EC mechanism was observed for the oxidation of dopamine at both ta-C and GC electrodes and the formation of polydopamine was suspected to cause the passivation of the electrodes.

Keywords

tetrahedral amorphous carbon, glassy carbon, dopamine, catechol, polydopamine, cyclic voltammetry

Introduction

Quinones are naturally occurring molecules in the human body. They can be found as free quinones, protein cofactors and in the mitochondrial electron transfer chain. Interestingly, quinones can also form toxins through electrochemical reactions, causing several cytotoxic effects in the body [1]. In addition, the electrochemistry of the catechol/quinone pair has importance in the electrochemical detection of several neurotransmitters such as dopamine and adrenaline that have a readily oxidizing hydroquinone moiety [2, 3].

Dopamine (DA) is one of the most important neurotransmitters in the brain, affecting cognitive, behavioral and motor functions. Abnormal dopamine transmission has been associated with several neurological disorders such as Parkinson's disease, schizophrenia, ADHD and Huntington's disease. [4] In order to understand the underlying role of dopamine in neurological functions and diseases, it is important to accurately measure its concentration *in vivo*. Electrochemical sensors based on carbon materials have been used extensively in the detection of dopamine and neurotransmitters in general [5].

In vivo measurements pose several challenges: firstly, dopamine is present at very low concentrations while several other neurotransmitters, occurring at higher concentrations, interfere with its electrochemical detection; secondly, the release and uptake of dopamine at the neuron terminals occur in rapid transients on a sub-second timescale. [3] Thus, the sensor must not only be sensitive and selective, it must also have a fast response time. Lastly, the sensor needs to be biocompatible and resistant to biofouling to remain stable and reliable during long-term

implantation in living systems. The electrode material is a key factor in determining the performance of the sensor under these conditions.

Diamond-like carbon (DLC) has received increasing attention, because it has many attractive properties for electrochemical sensor applications: chemical inertness, wide potential window, low background current and excellent mechanical properties [6-8]. DLC films can be deposited at room temperature allowing the use of a wide array of substrate materials and making it compatible with modern micro- and nanofabrication processes. [8] For *in vivo* use, DLC has also good biocompatibility [9] and resistance to bacterial adhesion [10]. Despite its potential, only few studies have investigated the application of DLC in the detection of neurotransmitters [11-13].

Recently, tetrahedral amorphous carbon (ta-C), a form of highly sp^3 -bonded, undoped DLC, was shown to be able to detect dopamine and possess favorable properties to be used as a substrate for *in vivo* electrodes [14, 15]. More importantly, it was shown that it is possible to build on top of ta-C hybrid carbon structures that exhibit very good selectivity and excellent sensitivity toward dopamine [16, 17]. As ta-C forms a large part of these novel hybrid electrodes it is of utmost importance to understand the physicochemical properties of ta-C thin films in contact with electrolytes and neurotransmitters. However, the electrochemical behavior of neurotransmitters at ta-C electrodes has not been investigated in-depth and the role of ta-C in the electrochemical properties of the hybrid carbon electrodes is not known precisely. Thus, this work completes our in-depth characterization of ta-C materials carried out during the last two years [14, 16-21] and provides the necessary electrochemical information needed to proceed to work with the more complex hybrid carbon materials.

In this work, the electrochemical behavior of dopamine, catechol (CA) and methylcatechol (MC) was investigated at ta-C thin film electrodes. The reaction mechanisms of these molecules were studied by cyclic voltammetry (CV) with varying scan rates at different pH values in sulfuric acid

and phosphate-buffered saline (PBS) solutions. Since most carbon electrodes are prone to surface fouling [22], the rate and extent of passivation of ta-C were examined by scanning several consecutive cycles with CV and analyzing the surface by X-ray photoelectron spectroscopy (XPS). The results were compared to the oxidation of these compounds at glassy carbon (GC) electrodes.

Material and methods

Ta-C thin film preparation

Tetrahedral amorphous carbon electrodes were fabricated on p-type Si (100) wafers (Ultrasil) with 0.001–0.002 Ohm·cm resistivity. A titanium interlayer was deposited before the ta-C layer to enhance adhesion. All wafers were cleaned by standard RCA cleaning procedure before the deposition. Direct current magnetron sputtering (DC-MS) and dual-filtered cathodic vacuum arc (FCVA) deposition systems were used for titanium and carbon deposition, respectively. It is to be noted that both systems are installed in one deposition chamber. Samples were placed in a rotating holder (rotational velocity used was 20 rpm). The vacuum in the chamber was pumped down by dry scroll vacuum pump (Edwards XDS10) and by cryo pump (Cryo-Torr, Helix Technology Corporation). In order to achieve a low vacuum, a high vacuum throttle valve was used. The DC-MS system was equipped with a circular, water-cooled magnetron sputtering source with a 2 inch Ti target (Kurt J. Lesker Company) and a DC generator (DCO2 BP). The shutter was utilized for controlling the sputtering time. Pre-sputtering of 2 min was carried out for cleaning the surface of the Ti target. Titanium interlayers were deposited under the following deposition conditions: discharge power was fixed at 100 W, total pressure was 0.67 Pa, Ar gas flow rate was 28 sccm, deposition temperature was close to room temperature and deposition time was 350 s. The FCVA system (Lawrence Berkeley National Laboratory) was equipped with a 60° bent magnetic filter for the reduction of the macroparticle contamination. Two 99.997 % graphite rods (Goodfellow) with a diameter of 6.35 mm were used as the carbon cathodes and they were surrounded by a cylindrical anode. The arc current pulses had an amplitude of 0.7 kA and pulse width of 0.6 ms. Each pulse was triggered at 1 Hz frequency. The 2.6 mF capacitor bank was charged to 400 V. The number of pulses was 360. The distance between the substrate holder and the filter was about 20 cm. Total pressure during the deposition process was no less than 1.3×10^{-4} Pa.

Cyclic Voltammetry

Cyclic voltammetry (CV) was carried out with a μ Autolab type III potentiostat (Metrohm Autolab). The reference electrode was an Ag/AgCl reference electrode (+0.197 V vs SHE) (Crison Instruments) and a platinum wire was used as the counter electrode. Only new ta-C electrodes and freshly polished GC electrodes were used for each measurement. GC electrodes with a diameter of 3 mm were polished with a 0.05 μ m alumina polishing suspension (Buehler) for 3 min, sonicated in distilled water for 5 min and thoroughly rinsed in distilled water before each experiment.

Catechol (Sigma-Aldrich), 4-methylcatechol (Sigma-Aldrich) and dopamine hydrochloride (Alfa Aesar, Johnson Matthey Company) were dissolved in either 0.5 M H₂SO₄ (Merck Suprapur) or 0.1 M PBS. The concentration of the catechols was always 1 mM. Neutral PBS (pH 7.2) was prepared from 0.05 M NaH₂PO₄ and 0.05 M Na₂HPO₄ (Sigma-Aldrich) and basic PBS (pH 10.8) from 0.05 M Na₂HPO₄ and 0.1 M NaOH. The pH of the H₂SO₄ solution was 0.65. pH values were measured with a Crison Basic 20+ pH-meter.

All the solutions were deoxygenated with argon for at least 10 min prior to measurements and the atmosphere in the electrochemical cell was purged during the experiments. All the measurements were conducted at room temperature. The cyclic voltammograms were recorded at scan rates of 10, 50, 200, 500 and 1000 mV/s. The peak current ratios were calculated from the baseline-corrected value of the reduction peak.

X-ray photoelectron spectroscopy (XPS)

The surface composition of the ta-C samples was analyzed with an SSX-100 ESCA in ultra-high vacuum using Al-K α irradiation (1486.6 eV). The fitting of the C 1s peaks was done using three components with a mixture of 80% Gaussian and 20% Lorentzian. The first component at 284.4 eV corresponded to sp² carbon atoms, the second at 285.3 eV to sp³ and the third component at 287.1 eV to other carbon bonds [23, 24].

Results and Discussion

Physical and chemical characterization of ta-C

The tetrahedral amorphous carbon (ta-C) thin films used in this study have been characterized in detail previously [14]. Here, we briefly summarize the main findings. The surface of ta-C was smooth with an average surface roughness of 1.6 ± 0.25 nm defined by atomic force microscopy (AFM). Transmission electron microscope (TEM) micrographs showed that the ta-C layer was completely amorphous and it was confirmed by X-ray reflectivity (XRR) and electron energy loss spectroscopy (EELS) measurements that the ta-C contained a high amount of sp^3 -bonded carbon.

The XPS results for ta-C are summarized in Table 1. For the ta-C samples that had not undergone cyclic voltammetry (samples 1 and 2), the atomic weight percent (at%) of sp^2 -bonded carbon was approximately 48 at%, that of sp^3 -bonded carbon 32 at% and other carbon bonds such as C-O bonds accounted for about 8 at%. The ta-C samples contained a relatively high amount of oxygen, roughly 10 at%. Small amounts of nitrogen (about 1 at%) as well as titanium and silicon from the substrate layers were also evident. Nitrogen was present in the vacuum chamber and was most likely introduced in the samples during the deposition procedure. Based on the zeta potential measurement that gave an isoelectric point of pH 2.6 [14] and on the amount of oxygen in the XPS measurements, the surface of ta-C most likely contained acidic functional groups such as carboxyl and hydroxyl groups. This finding was also consistent with the X-ray absorption spectroscopy (XAS) results that confirmed that about 20% of the volume of the sample surface (within the present sampling depth) was composed of hydroxyl, carboxyl, carbonyl and C-O-C bonds [25].

Catechol/quinone redox system

The structures of catechol, methylcatechol and dopamine are shown in Fig. 1. These three catechols oxidize to the corresponding ortho-quinones in a two-electron, two-proton transfer process. The order of proton and electron transfer follows the scheme of squares, presented in Fig. 2, and is

dependent on pH. This model assumes that protonations are at equilibrium and that the electron transfer step is rate-determining. [26-28] The proposed electron and proton transfer sequence at neutral pH is H^+ , e^- , H^+ , e^- and it is illustrated in red in the scheme of squares in Fig. 2. This transfer sequence has been suggested for hydroquinone on platinum [26] and for methylcatechol, 3,4-dihydroxybenzylamine (DHBA) and 3,4-dihydroxyphenylacetic acid (DOPAC) on carbon paste electrodes [27, 28]. Since DA is structurally very similar to DHBA (Fig. 1), it most likely follows the same reaction sequence.

The pK_a values for CA, MC, and DA are listed in Table 2. The first two pH values used in this study (0.65 and 7.2) are below pK_{a5} of all three catechols, so the transfer sequence in the scheme of squares starts from the fully protonated form of the catechol, QH_2 . The last pH value of 10.8 is between pK_{a5} and pK_{a6} , therefore the starting point for the reaction is the deprotonated form QH^- .

As opposed to outer-sphere redox systems, the electrode surface is known to drastically affect catechol voltammetry [5, 22, 35-37]. It has in fact been questioned whether the scheme of squares can be applied to all electrode substrates owing to the wide variety of carbon electrode materials and numerous surface preparation methods [36].

Adsorption also plays a crucial role in the fast electron transfer of catechols. It has been shown that the surface modification of GC by an inert monolayer effectively prevents catechol adsorption and adversely or completely inhibits electron transfer. [35, 36] However, if the adsorbed layer is formed by a quinone, catechol electron transfer is only slightly affected even if adsorption of the catechol is apparently blocked [36]. Furthermore, it has been reported that the adsorption process of dopamine on platinum is sensitive to crystallographic orientation [38]. These findings further emphasize the importance of electrode surface properties on the adsorption and oxidation of catechols.

Oxidation of catechol

The cyclic voltammograms of catechol in H₂SO₄ (pH 0.65) and PBS (pH 7.2 and 10.8) are shown in Fig. 3. In neutral PBS, the oxidation peak of catechol occurs at +0.43 V, while the corresponding reduction peak is near +0.01 V using a scan rate of 50 mV/s. The peak potential separation, ΔE_p , is thus 0.42 V. It can be observed from Table 3 that ΔE_p changes as a function of scan rate, indicating a quasi-reversible redox system. Similar behavior is observed also in H₂SO₄ and basic PBS. The large ΔE_p values imply sluggish electron transfer kinetics at the ta-C electrode.

After the first scan, there is a considerable increase in ΔE_p and decrease in peak currents at neutral pH. This behavior is observed at all scan rates, but it is less adverse at high scan rates and vice versa. Also, the peak current ratio, I_{red} / I_{ox} (Table 3), deviates significantly from unity at all scan rates, implicating a coupled homogeneous reaction or a complication in the electron transfer process [39]. It is known that at neutral pH the oxidation of catechol is accompanied by hydroxylation and polymerization reactions. The ortho-quinone can undergo a nucleophilic attack by water to yield a hydroxylated derivative such as a 1,2,4-trihydroxybenzene [40, 41] or it can form a dimer with a catechol and polymerize [42]. The shoulder observed after the CA oxidation peak is likely due to the oxidation of one of the products formed in the chemical reactions (no oxidation peak is seen in pure PBS).

The polymerization product is most probably the cause of the electrode surface fouling and leads to the slower electron transfer kinetics and lower peak currents observed after the first scan. Polycatechol films have been reported on glassy carbon [43] and gold [44] electrodes and have been suspected to be the cause of fouling also on boron-doped diamond [45].

At pH 10.8 in PBS, the oxidation peak is shifted to more negative potentials, at +0.03V, since the deprotonation step in the scheme of squares is pH dependent [26-28, 46]. The reduction peak of the ortho-quinone is not observed at slow scan rates and clearly appears only at a scan rate of 200 mV/s, increasing in magnitude at faster scan rates. This indicates the occurrence of an irreversible

chemical reaction coupled to the oxidation of catechol. At slow scan rates the ortho-quinone is totally consumed by the chemical reaction and no reduction peak is seen. The hydroxylation reaction has been shown to be quite rapid at high pH because of the abundance of hydroxyl ions that can attach to the o-quinone ring by nucleophilic addition [40]. The observed rate constant for dimerization also increases in more alkaline solutions [42], which could explain why the electron transfer is more adversely inhibited at pH 10.8 than in neutral PBS (both in terms of ΔE_p and peak current magnitude as can be seen from Fig. 3). The shoulder following the oxidation peak is present at all scan rates and could possibly correspond to the oxidation of one of the products formed in the chemical reactions. This possible oxidation product is not reduced within the investigated potential window, however.

In H_2SO_4 , the redox peaks are shifted to more positive values compared to neutral PBS. The oxidation peak is found at +0.7 V and the reduction peak at +0.34V. The voltammetric response in H_2SO_4 deteriorates significantly less than in neutral and basic solutions even if the peak current ratio still greatly deviates from unity (Table 3). Thus, the polymerization must be inhibited or prevented and another irreversible chemical reaction most likely accounts for the low I_{red} / I_{ox} value. Additionally, no shoulder resulting from hydroxylation or polymerization products is seen after the oxidation peak of catechol.

Oxidation of methylcatechol

The electrochemical response of methylcatechol at ta-C electrodes is similar to that of catechol as can be seen from Fig. 4. In neutral PBS, the oxidation peak of MC is seen at +0.29 V and the reduction peak at -0.01 V. The ΔE_p values, given in Table 4, change as a function of scan rate indicating a quasi-reversible process with slow electron transfer kinetics. The redox peaks shifted to more negative potentials as pH increased and vice versa.

In spite of the similar behavior, the ΔE_p values indicate that the electron transfer of MC is faster than that of CA at the ta-C electrode. Especially in H_2SO_4 and neutral PBS, the ΔE_p values are significantly lower. However, deterioration of the electrochemical response still occurs at approximately the same rate as with catechol, which can be seen from the change in ΔE_p over the course of 10 consecutive cycles as shown in Figure 5. The peak currents also diminish as the scanning progresses. The ΔE_p values at 50 and 500 mV/s seem to reach the same final value after scanning 10 cycles, corresponding possibly to the full extent of passivation of the electrode surface. In the same way as catechol, methylcatechol can also undergo hydroxylation and dimerization reactions after being oxidized to the o-quinone [40, 47]. The shoulders that are seen on the CVs after the oxidation peak are likely due to the oxidation of the compounds resulting from these coupled chemical reactions. Again, note that this possible oxidation product is not reduced within the investigated potential window, as was the case with CA.

The deterioration of the electrode kinetics is slight in H_2SO_4 , while it is marked in neutral and alkaline PBS. At pH 10.8, the increase in ΔE_p values was most significant and the I_{red} / I_{ox} ratios deviated most from unity. The coupled chemical reaction is clearly irreversible, since no reduction peak was observed below 50 mV/s and its magnitude increased at faster scan rates. As it was seen previously with CA, the hydroxylation and dimerization reactions appear to be very fast at high pH and slow down considerably at low pH. [40].

Comparing the behavior of CA and MC, the slight differences are most likely related to the methyl group in methylcatechol. It could protect the aromatic ring from nucleophilic attack in position 4 and possibly provide some steric hindrance against the formation of the polymer layer. In addition, the CH_3 group could explain the lower ΔE_p values in comparison to CA. It has been suggested that substitution of electron-donating groups such as CH_3 renders certain aromatic compounds more easily oxidizable [31, 48].

Oxidation of dopamine

The cyclic voltammograms of dopamine are shown in Fig. 6. In neutral PBS at a scan rate of 50 mV/s, the oxidation peak appears at +0.39 V and the reduction peak at 0.00 V. The magnitude of the reduction peak is very small and the $I_{\text{red}}/I_{\text{ox}}$ value is only 0.11 (Table 5). This behavior is explained by a coupled chemical reaction in which the dopamine o-quinone undergoes an intramolecular cyclization via 1,4-Michael addition with its amine side chain to form leucodopaminechrome (LDAC) [49-51]. At very slow scan rates, the o-quinone is completely consumed in the chemical reaction before it is reduced back to dopamine and therefore reduction does not occur at all. However, a scan rate of 50 mV/s is fast enough so that a small reduction peak is observed. An additional reduction peak appears at -0.5 V on the first scan corresponding to the reduction of dopaminechrome (DAC) to leucodopaminechrome (LDAC). On the subsequent scan, the corresponding oxidation of leucodopaminechrome can be seen at +0.06 V.

In the case of CA and MC, the o-quinone undergoes nucleophilic attack by H₂O, but the side chain intracyclization of dopamine is three orders of magnitude faster than the rate of addition of H₂O to dopaminequinone [50]. Therefore, any nucleophilic reaction is largely overrun by the faster intracyclization. In H₂SO₄, however, the intracyclization is prevented because at low pH the amino side chain is protonated [49, 51, 52], which also explains why the dopaminechrome redox pair is not seen in the CVs. Therefore, the hydroxylation reaction may be feasible also for DA in acidic medium. Despite the fact that this reaction has been suggested to be very slow on the time-scale of cyclic voltammetry at low pH [50], the large deviation of peak current ratio from 1 indicates that it may still play some role when the faster intracyclization is prevented.

The reaction pathway in neutral PBS can be defined as an ECE mechanism and it has been reported to take place for catecholamines on carbon electrodes [49, 51] as well as gold [52] and platinum [38]. In addition, an ECC mechanism in which leucodopaminechrome is reduced by dopamine o-

quinone to dopaminechrome has been suggested [49, 50, 53]. It is well established that dopaminechrome (DAC) further reacts to form a melanin-like polymer [51, 52]. According to the ECECE mechanism proposed by Li et al. for the formation of this polymer film on gold electrodes, dopaminechrome (DAC) is first isomerized to 5,6-dihydroxyindole, then oxidized to 5,6-indolequinone which is in turn oxidized to poly(5,6-indolequinone) [52]. Self-polymerization of dopamine in alkaline aqueous solutions to form polydopamine films has been shown to occur on a wide variety of substrate materials [54]. The exact mechanism of polydopamine formation is still debated in literature. However, all the proposed mechanisms involve the indolequinone as a building block that is either covalently or non-covalently bonded (or a mixture of both types of bonds) to other monomers. Properties of polydopamine and its polymerization mechanisms have been recently reviewed in detail [55].

The formation of polydopamine is the most probable cause of the severe passivation of the ta-C electrodes seen in neutral and alkaline solutions in Fig. 6. A significant increase in ΔE_p (see also Fig. 8) and a decrease in peak currents can be noticed in only a few cycles until all the peaks flatten at slow scan rates. The XPS data in Table 1 also shows a significant increase in nitrogen for samples that have been cycled at either 10 or 50 mV/s in PBS (pH 7.2 or 10.9). This nitrogen is attributed to the amine group in dopamine, since the PBS solutions do not contain this element. At high scan rates in neutral PBS (Fig. 6 E), the intramolecular cyclization does not have time to occur and the passivation is less significant. This can be seen from the clear reduction peak of dopaminequinone and consequently higher I_{red}/I_{ox} ratio at higher scan rates. Additionally, the redox peaks of the dopaminechrome pair become less discernible as seen in Fig. 6 E. Thus, the intramolecular cyclization can be avoided by increasing scan rate. However, in alkaline pH, the coupled chemical reaction is so fast that increasing the scan rate to 1000 mV/s does not prevent it from taking place. Furthermore, the reduction of dopaminequinone is not seen at all even at fast

scan rates (Fig. 6 F). Oxidation peaks at around +1.0 V are attributed to the oxidation of products formed in the polymerization process of DA.

In H₂SO₄, the electrochemical behavior of dopamine (Fig. 6 A and D) is very similar to that of catechol and methylcatechol because, as mentioned previously, the intracyclization is inhibited. The oxidation of DA to dopaminequinone occurs at +0.65 V and the reduction at +0.39 V (50 mV/s), and no other redox peaks are observed. The electron transfer kinetics are slow and the process is quasi-reversible. The peak potential separation and peak current magnitude do not change severely over the course of 10 consecutive cycles, thus polymerization reactions do not seem to occur extensively. However, the $I_{\text{red}} / I_{\text{ox}}$ ratio of 0.58 (Table 5) suggests that a coupled homogeneous reaction follows the oxidation of dopamine even at low pH.

While considering the results of the passivation studies above, it should be noted that the polymerization of dopamine is prevented in the central nervous system because physiological reducing agents, such as ascorbic acid, reduce dopaminequinone back to its original form before the intracyclization can occur [51]. Therefore the deterioration of electrode kinetics reported here does not apply directly to conditions in the central nervous system. Furthermore, passivation is much less severe at low concentration of dopamine such as in the brain, because less oxidation products are accumulated at the surface of the electrode [22].

Comparison with glassy carbon

Since the electrochemical reactions of different catechols have been studied extensively on glassy carbon, the present results obtained at ta-C electrodes were compared to those acquired at GC electrodes. Only data at neutral pH was considered. The cyclic voltammograms at 50 mV/s are presented in Figure 7 and the ΔE_p and $I_{\text{red}} / I_{\text{ox}}$ values are calculated in Table 6. The ΔE_p values are in agreement with those found in literature [35, 36]. The redox reactions on GC are considerably

more reversible than on ta-C. The peak potential separation still shows a dependency on scan rate and the reactions of all three catechols are quasi-reversible as at ta-C electrodes.

The $I_{\text{red}} / I_{\text{ox}}$ ratios are close to unity at all scan rates for methylcatechol and there is slight deviation only at 10 mV/s for catechol. However, the $I_{\text{red}} / I_{\text{ox}}$ ratios deviate considerably for dopamine indicating a coupled chemical reaction that is very marked at slow scan rates. In Fig. 7 C, the second redox pair attributed to dopaminechrome is clearly visible and thus the same EC mechanism is observed on both GC and ta-C. However, the redox peaks are much more reversible and well-defined on GC.

Some deterioration of the electrode kinetics is seen particularly at slow scan rates, whereas at fast scan rates it is much more negligible than on ta-C. The change in ΔE_p values over ten cycles at ta-C and GC electrodes are shown in Fig. 8 for comparison. The difference in the reversibility of the dopamine redox reaction is obvious as well as the difference in the rate of passivation between the two electrodes.

Observed trends

In this section some general trends that were observed in the experiments are illustrated. The plots of $\log(I_{\text{ox}})$ vs $\log(v)$ are presented in Fig. 9 for all three catechols. The slope for a diffusion-controlled process should be 0.5 and for an adsorption-controlled process it should be 1 [39]. The slopes, given in Table 7, are very close to 0.5 at neutral and acidic pH, while at more alkaline pH they are significantly lower than 0.5 for all three of the catechols. Thus, it can be concluded that at neutral and acidic pH the oxidation reactions of CA, MC and DA are all more or less under diffusion control. In the literature it has been demonstrated that the adsorption of catechols is necessary for the electron transfer reactions to occur [35, 36]. This is, however, not in disagreement with the present results since the fact that adsorption is required in the oxidation does not necessarily mean that it is the rate determining step.

Plots of the oxidation peak potential E_{ox} versus pH are shown in Fig. 10 and the corresponding slopes are given in Table 7. The experimental data gives slopes that are very close to -59 mV per pH unit which is consistent with a 2-electron and 2-proton transfer mechanism at pH values below 9. Similar results have been reported in literature [46, 50].

In Figure 11, the ΔE_p values are plotted versus pH. The peak potential separations at pH 0.65 and 10.8 are clearly smaller than at neutral pH and indicate that electron transfer is slowest around neutral pH for all the catechols. From Figure 12 it can be seen that neutral pH also corresponds to the lowest I_{ox} values, so the extent of oxidation of the catechols is lowest around pH 7.2. Consistent with the trend seen in oxidation peak currents, the peak current ratios I_{red} / I_{ox} show the highest values at pH 7.2 for CA and MC (Fig. 13). Dopamine, however, behaves differently due to the intramolecular cyclization that occurs very rapidly at neutral and alkaline pH. The value of I_{red} / I_{ox} is therefore heavily dependent on the scan rate. At slow scan rates, dopaminequinone is consumed completely and no reduction occurs. Thus, the I_{red} / I_{ox} ratio is lower at neutral than at acidic pH. At high scan rates the reduction occurs and the peak current ratio is again higher than at pH 0.65. The reduction peak is not observed at all at pH 10.8 due to the rapidity of the chemical reaction.

Conclusion

The electrochemical response of catechol, methylcatechol and dopamine was investigated at ta-C electrodes. It was shown that all of these redox systems exhibited quasi-reversible behavior with sluggish electron transfer kinetics and the reactions were apparently diffusion-controlled. At neutral and alkaline pH, coupled homogeneous reactions followed the oxidation to the ortho-quinone and led to significant deterioration of the electrode response. At acidic pH, the extent of deterioration was considerably lower. An EC mechanism was observed for the oxidation of dopamine at both ta-C and GC electrodes and the formation of polydopamine passivated the electrodes. The redox

reactions of all three catechols showed faster electron transfer kinetics at GC electrodes and GC was less susceptible toward surface fouling than ta-C.

Despite the several advantages attributed to ta-C in electrochemical sensor applications, ta-C by itself is not well suited for the detection of DA because of its slow electron transfer kinetics for catechol redox systems associated with poor selectivity and sensitivity toward dopamine [14]. Future work will investigate the electrochemical behavior of dopamine at hybrid carbon electrodes where ta-C has been used as a substrate material.

Acknowledgements

Authors wish to acknowledge the financial support by the Finnish Parkinson Foundation (T.P), the Finnish Funding Agency for Innovation (grant number 211488) (T.P., S.S. and T.L.), the Academy of Finland (grant number 285015) (T.L.) and MINECO project CTQ2013-44083-P (J.F.M.).

References

- [1] Bolton, J.L., Trush, M.A., Penning, T.M., Dryhurst, G., Monks, T.J. Role of Quinones in Toxicology. *Chemical Research in Toxicology*, 2000, vol. 13, pp. 135-160.
- [2] Adams, R.N. Probing brain chemistry with electroanalytical techniques. *Analytical Chemistry*, 1976, vol. 48, pp. 1126A-1138A.
- [3] Robinson, D.L., Hermans, A., Seipel, A.T., Wightman, R.M. Monitoring Rapid Chemical Communication in the Brain. *Chemical Reviews*, 2008, vol. 108, pp. 2554-2584.
- [4] Beaulieu, J., Gainetdinov, R.R. The Physiology, Signaling, and Pharmacology of Dopamine Receptors. *Pharmacological Reviews*, 2011, vol. 63, pp. 182-217.
- [5] McCreery, R.L. Advanced Carbon Electrode Materials for Molecular Electrochemistry. *Chemical Reviews*, 2008, vol. 108, pp. 2646-2687.
- [6] Robertson, J. Diamond-like amorphous carbon. *Materials Science and Engineering: R: Reports*, 2002, vol. 37, pp. 129-281.
- [7] Compton, R., Foord, J., Marken, F. Electroanalysis at Diamond-Like and Doped-Diamond Electrodes. *Electroanalysis*, 2003, vol. 15, pp. 1349-1363.
- [8] Zeng, A., Neto, V.F., Gracio, J.J., Fan, Q.H. Diamond-like carbon (DLC) films as electrochemical electrodes. *Diamond and Related Materials*, 2014, vol. 43, pp. 12-22.
- [9] Kaivosoja, E., Suvanto, P., Barreto, G., Aura, S., Soininen, A., Franssila, S., Konttinen, Y.T. Cell adhesion and osteogenic differentiation on three-dimensional pillar surfaces. *Journal of Biomedical Materials Research Part A*, 2013, vol. 101A, pp. 842-852.
- [10] Levon, J., Myllymaa, K., Kouri, V.P., Rautemaa, R., Kinnari, T., Myllymaa, S., Konttinen, Y. T., Lappalainen, R. Patterned macroarray plates in comparison of bacterial adhesion inhibition of

tantalum, titanium, and chromium compared with diamond-like carbon. *Journal of Biomedical Materials Research Part A*, vol. 92A, pp. 1606-1613, 2010.

[11] Sopchak, D., Miller, B., Kalish, R., Avyigal, Y., Shi, X. Dopamine and Ascorbate Analysis at Hydrodynamic Electrodes of Boron Doped Diamond and Nitrogen Incorporated Tetrahedral Amorphous Carbon. *Electroanalysis*, 2002, vol. 14, pp. 473-478.

[12] Tanaka, Y., Naragino, H., Yoshinaga, K., Nakahara, A., Kondo, T., Fujishima, A., Honda, K. Controllable Electrochemical Activities by Oxidative Treatment toward Inner-Sphere Redox Systems at N-Doped Hydrogenated Amorphous Carbon Films. *International Journal of Electrochemistry*, 2011, vol. 2012.

[13] Medeiros, R.A., Benchick, A., Rocha-Filho, R.C., Fatibello-Filho, O., Saidani, B., Debiemme-Chouvy, C., Deslouis, C. Simultaneous detection of ascorbic acid and dopamine with electrochemically pretreated carbon nitride electrodes: Comparison with boron-doped diamond electrodes. *Electrochemistry Communications*, 2012, vol. 24, pp. 61-64.

[14] Laurila, T., Protopopova, V., Rhode, S., Sainio, S., Palomäki, T., Moram, M., Feliu, J.M., Koskinen, J. New electrochemically improved tetrahedral amorphous carbon films for biological applications. *Diamond and Related Materials*, 2014, vol. 49, pp. 62-71.

[15] Kaivosoja, E., Sainio, S., Lyytinen, J., Palomäki, T., Laurila, T., Kim, S.I., Han, J.G., Koskinen, J. Carbon thin films as electrode material in neural sensing. *Surface and Coatings Technology*, 2014, vol. 259, Part A, pp. 33-38.

[16] Sainio, S., Palomäki, T., Rhode, S., Kauppila, M., Pitkänen, O., Selkälä, T., Toth, G., Kordas, K., Moram, M., Koskinen, J. and Laurila T. Carbon Nanotube (CNT) Forest on Diamond-like Carbon (DLC) Electrode Improves Electrochemical Sensitivity Towards Dopamine by Two Orders of Magnitude, *Sensors and Actuators B*, 2015, vol. 211, pp.177-186.

- [17] Sainio, S., Palomäki, T., Tujunen, N., Protopopova, V., Koehne, J., Kordas, K., Koskinen, J., Meyyappan, M. and Laurila, T. Integrated Carbon Nanostructures for Detection of Neurotransmitters. *Molecular Neurobiology*, 2015, pp. 1-8.
- [18] Protopopova, V., Iyer, A., Wester, N., Kondrateva, A., Sainio, S., Palomäki, T., Laurila, T., Mishin, M., and Koskinen J. Ultrathin undoped tetrahedral amorphous carbon films: The role of the underlying titanium layer on the electronic structure, *Diamond and Related Materials*, 2015, vol. 57, pp. 43-52.
- [19] Protopopova, V., Wester, N., Caro, M., Gabdullin, P., Palomäki, T., Laurila, T. and Koskinen, J. Ultrathin undoped tetrahedral amorphous carbon films: Thickness dependence of the electronic structure and implications to electrochemical behavior, *Physical Chemistry Chemical Physics*, 2015, vol. 17, pp. 9020-9031.
- [20] Caro, M., Zoubkoff, R., Lopez-Acevedo, O. and Laurila, T. Atomic and electronic structure of tetrahedral amorphous carbon surfaces from density functional theory: properties and simulation strategies, *Carbon*, 2014, vol. 77, pp. 1168-1182.
- [21] Caro, M., Määttä, J., Lopez-Acevedo, O. and Laurila T. Energy band alignment and electronic states of amorphous carbon surfaces in vacuo and in aqueous environment, *Journal of Applied Physics*, 2015, vol. 117, pp. 034502.
- [22] Patel, A.N., Tan, S., Miller, T.S., Macpherson, J.V., Unwin, P.R. Comparison and Reappraisal of Carbon Electrodes for the Voltammetric Detection of Dopamine. *Analytical Chemistry*, 2013, vol. 85, pp. 11755-11764.

- [23] Díaz, J., Paolicelli, G., Ferrer, S., Comin, F. Separation of the sp³ and sp² components in the C1s photoemission spectra of amorphous carbon films. *Physical Review B*, 1996, vol. 54, pp. 8064-8069.
- [24] Merel, P., Tabbal, M., Chaker, M., Moisa, S., Margot, J. Direct evaluation of the sp³ content in diamond-like-carbon films by XPS. *Applied Surface Science*, 1998, vol. 136, pp. 105-110.
- [25] Sainio, S., Nordlund, D., Koehne, J., Meyyappan, M., Koskinen, J., Laurila, T. Unpublished results.
- [26] Laviron, E. Electrochemical reactions with protonations at equilibrium: Part X. The kinetics of the p-benzoquinone/hydroquinone couple on a platinum electrode. *Journal of Electroanalytical Chemistry and Interfacial Electrochemistry*, 1984, vol. 164, pp. 213-227.
- [27] Deakin, M.R., Kovach, P.M., Stutts, K.J., Wightman, R.M. Heterogeneous mechanisms of the oxidation of catechols and ascorbic acid at carbon electrodes. *Analytical Chemistry*, 1986, vol. 58, pp. 1474-1480.
- [28] Deakin, M.R., Wightman, R.M. The kinetics of some substituted catechol/o-quinone couples at a carbon paste electrode. *Journal of Electroanalytical Chemistry and Interfacial Electrochemistry*, 1986, vol. 206, pp. 167-177.
- [29] Land, E.J., Porter, G., Strachan, E. Primary photochemical processes in aromatic molecules. Part 6. - The absorption spectra and acidity constants of phenoxy radicals. *Transactions of the Faraday Society*, 1961, vol. 57, pp. 1885-1893.
- [30] Steenken, S., O'Neill, P. Oxidative demethoxylation of methoxylated phenols and hydroxybenzoic acids by the hydroxyl radical. An in situ electron spin resonance, conductometric pulse radiolysis and product analysis study. *The Journal of Physical Chemistry*, 1977, vol. 81, pp. 505-508.

- [31] Steenken, S., Neta, P. Electron transfer rates and equilibria between substituted phenoxide ions and phenoxyl radicals. *The Journal of Physical Chemistry*, 1979, vol. 83, pp. 1134-1137.
- [32] Richter, H.W., Waddell, W.H. Mechanism of the oxidation of dopamine by the hydroxyl radical in aqueous solution. *Journal of the American Chemical Society*, 1983, vol. 105, pp. 5434-5440.
- [33] Martin, R.B. Zwitterion formation upon deprotonation in L-3,4-dihydroxyphenylalanine and other phenolic amines. *The Journal of Physical Chemistry*, 1971, vol. 75, pp. 2657-2661.
- [34] Kiss, T., Sovago, I., Martin, R.B. Complexes of 3,4-dihydroxyphenyl derivatives. 9. Aluminum(3+) binding to catecholamines and tiron. *Journal of the American Chemical Society*, 1989, vol. 111, pp. 3611-3614.
- [35] DuVall, S.H., McCreery, R.L. Control of Catechol and Hydroquinone Electron-Transfer Kinetics on Native and Modified Glassy Carbon Electrodes. *Analytical Chemistry*, 1999, vol. 71, pp. 4594-4602.
- [36] DuVall, S.H., McCreery, R.L. Self-catalysis by Catechols and Quinones during Heterogeneous Electron Transfer at Carbon Electrodes. *Journal of the American Chemical Society*, 2000, vol. 122, pp. 6759-6764.
- [37] Banks, C.E., Davies, T.J., Wildgoose, G.G., Compton, R.G. Electrocatalysis at graphite and carbon nanotube modified electrodes: edge-plane sites and tube ends are the reactive sites. *Chemical Communications (Cambridge, England)*, 2005, vol. (7), pp. 829-841.
- [38] Chumillas, S., Figueiredo, M.C., Climent, V., Feliu, J.M. Study of dopamine reactivity on platinum single crystal electrode surfaces. *Electrochimica Acta*, 2013, vol. 109, pp. 577-586.

- [39] Bard, A.J., Bard, A.J. and Faulkner, L.R. *Electrochemical Methods: Fundamentals and Applications*. New York (N.Y.), Wiley, 2000.
- [40] Papouchado, L., Petrie, G. and Adams, R.N. Anodic oxidation pathways of phenolic compounds: Part I. Anodic hydroxylation reactions. *Journal of Electroanalytical Chemistry and Interfacial Electrochemistry*, 1972, vol. 38, pp. 389-395.
- [41] Cabaniss, G.E., Diamantis, A.A., Murphy, W.R., Linton, R.W., Meyer, T.J. Electrocatalysis of proton-coupled electron-transfer reactions at glassy carbon electrodes. *Journal of the American Chemical Society*, 1985, vol. 107, pp. 1845-1853.
- [42] Ryan, M.D., Yueh, A., Chen, W. The Electrochemical Oxidation of Substituted Catechols. *Journal of the Electrochemical Society*, 1980, vol. 127, pp. 1489-1495.
- [43] Qian, G., Yang, C., Pu, W., Huang, J. and Zhang, J. A novel polycatechol/platinum composite film prepared by electrochemical synthesis. *Synthetic Metals*, 2007, vol. 157, pp. 448-453.
- [44] Barham, A.S., Kennedy, B.M., Cunnane, V.J., Daous, M.A. The Electrochemical polymerisation of 1,2 dihydroxybenzene and 2-hydroxybenzyl alcohol prepared in different solutions media. *Electrochimica Acta*, 2014, vol. 147, pp. 19-24.
- [45] Nasr, B., Gadri, A., Canizares, P., Saez, C., Lobato, J., Rodrigo, M.A. Electrochemical Oxidation of Hydroquinone, Resorcinol, and Catechol on Boron-Doped Diamond Anodes. *Environmental Science & Technology*, 2005, vol. 39, pp. 7234-7239.
- [46] Lin, Q., Li, Q., Batchelor-McAuley, C. and Compton, R.G. Two-Electron, Two-Proton Oxidation of Catechol: Kinetics and Apparent Catalysis. *The Journal of Physical Chemistry C*, 2015, vol. 119, pp. 1489-1495.

- [47] Adams, R.N., Hawley, M.D. and Feldberg, S.W. Nuances of the E.C.E. mechanism. II. Addition of hydrochloric acid and amines to electrochemically generated o-benzoquinones. *The Journal of Physical Chemistry*, 1967, vol. 71, pp. 851-855.
- [48] Steenken, S. and Neta, P. One-electron redox potentials of phenols. Hydroxy- and aminophenols and related compounds of biological interest. *The Journal of Physical Chemistry*, 1982, vol. 86, pp. 3661-3667.
- [49] Hawley, M.D., Tatawawadi, S.V., Piekarski, S. and Adams, R.N. Electrochemical Studies of the Oxidation Pathways of Catecholamines. *Journal of the American Chemical Society*, 1967, vol. 89, pp. 447-450.
- [50] Sternson, A.W., McCreery, R., Feinberg, B. and Adams, R.N. Electrochemical studies of adrenergic neurotransmitters and related compounds. *Journal of Electroanalytical Chemistry and Interfacial Electrochemistry*, 1973, vol. 46, pp. 313-321.
- [51] Tse, D.C.S., McCreery, R.L. and Adams, R.N. Potential oxidative pathways of brain catecholamines. *Journal of Medicinal Chemistry*, 1976, vol. 19, pp. 37-40.
- [52] Li, Y., Liu, M., Xiang, C., Xie, Q. and Yao, S. Electrochemical quartz crystal microbalance study on growth and property of the polymer deposit at gold electrodes during oxidation of dopamine in aqueous solutions. *Thin Solid Films*, 2006, vol. 497, pp. 270-278.
- [53] Gelbert, M., Curran, D. Alternating Current Voltammetry of Dopamine and Ascorbic Acid at Carbon Paste and Stearic Acid Modified Carbon Paste Electrodes. *Analytical Chemistry*, 1986, vol. 58, pp. 1028-1032.
- [54] Lee, H., Dellatore, S.M., Miller, W.M. and Messersmith, P.B. Mussel-Inspired Surface Chemistry for Multifunctional Coatings. *Science*, 2007, vol. 318, pp. 426-430.

[55] Liu, Y., Ai, K. and Lu, L. Polydopamine and Its Derivative Materials: Synthesis and Promising Applications in Energy, Environmental, and Biomedical Fields. *Chemical Reviews*, 2014, vol. 114, pp. 5057-5115.

ACCEPTED MANUSCRIPT

Figure captions

Figure 1. The structures of catechol, methylcatechol, dopamine and DHBA (3,4-dihydroxybenzylamine) at physiological pH.

Figure 2. The scheme of squares represents the possible electron and proton transfer sequences of catechols. The formal potentials (E^0) and heterogeneous reaction rate constants (k) affect electron transfer whereas pK_a values relate to the oxidation state of the molecule. The suggested transfer sequence at neutral pH on GC is illustrated in red.

Figure 3. Cyclic voltammograms of 1 mM CA in (A) 0.5 M H_2SO_4 (pH 0.65), (B) PBS (pH 7.2) and (C) PBS (pH 10.8) at ta-C electrodes. Scan rate 50 mV/s, 10 consecutive cycles.

Figure 4. Cyclic voltammograms of 1 mM MC in (A) 0.5 M H_2SO_4 (pH 0.65), (B) PBS (pH 7.2) and (C) PBS (pH 10.8) at ta-C electrodes. Scan rate 50 mV/s, 10 consecutive cycles.

Figure 5. Plots of ΔE_p as a function of cycle number for 1 mM CA and 1 mM MC at 50 mV/s and 500 mV/s in PBS (pH 7.2).

Figure 6. Cyclic voltammograms of 1 mM DA in (A) and (D) 0.5 M H_2SO_4 (pH 0.65); (B) and (E) PBS (pH 7.2); (C) and (F) PBS (pH 10.8). Upper row 50 mV/s, lower row 500 mV/s, 10 consecutive cycles.

Figure 7. Cyclic voltammograms of (A) 1 mM CA, (B) 1 mM MC, and (C) 1 mM DA in PBS (pH 7.2) at GC electrodes. Scan rate 50 mV/s, 10 consecutive cycles.

Figure 8. Plot of ΔE_p as a function of cycle number for 1 mM DA in PBS (pH 7.2) at ta-C and at GC electrodes. Scan rates: 50 mV/s and 500 mV/s. After the third cycle ΔE_p could not be calculated for the ta-C electrode because there was no reduction peak.

Figure 9. Plots of $\log(I_{ox})$ vs $\log(v)$ for (A) CA, (B) MC and (C) DA in 0.5 M H_2SO_4 (pH 0.65), PBS (pH 7.2) and PBS (pH 10.8).

Figure 10. Plots of E_{ox} vs pH for (A) CA, (B) MC and (C) DA at 10 mV/s, 50 mV/s and 500 mV/s.

Figure 11. Plots of ΔE_p as a function of pH for (A) CA, (B) MC and (C) DA. Scan rates: 50 mV/s (circles), 500 mV/s (triangles). ΔE_p could not be determined for DA in pH 10.8 because there was no reduction peak.

Figure 12. Plots of I_{ox} vs pH for (A) CA, (B) MC and (C) DA. Scan rates: 10 mV/s (squares), 50 mV/s (circles) and 500 mV/s (triangles).

Figure 13. Plots of I_{red}/I_{ox} vs pH for (A) CA, (B) MC and (C) DA. Scan rates: 50 mV/s (squares) and 500 mV/s (triangles). I_{red}/I_{ox} values could not be determined in pH 10.8 for DA because there was no reduction peak.

Tables

Table 1. XPS results showing the elemental composition of ta-C samples. Samples 1 and 2 are reference samples that did not undergo cyclic voltammetry. Samples 3 and 4 were scanned 10 cycles in 1 mM DA in PBS (pH 7.2) at a scan rate of 10 and 50 mV/s respectively. Samples 5 and 6 were scanned 10 cycles in 1 mM DA in PBS (pH 10.9) at a scan rate of 10 and 50 mV/s respectively.

Sample	Element (at%)							
	C (1s)	C (1s) sp ²	C (1s) sp ³	O (1s)	N (1s)	Ti (2p)	Si (2s)	Na (1s)
ta-C-1	7.2	46.7	32.0	12.0	1.1	0.29	0.67	-
ta-C-2	8.0	48.2	32.1	9.5	0.95	0.49	0.71	-
ta-C-3	9.3	36.0	24.6	22.7	6.5	0.07	0.4	0.3
ta-C-4	11.1	34.7	28.1	19.1	6.1	-	0.4	0.6
ta-C-5	10.0	43.5	21.1	18.2	4.9	-	0.4	
ta-C-6	11.1	28.6	34.6	18.7	5.8	-	0.2	0.8

Table 2. Assumed pK_a values for the three catechols examined.

	pK_{a1}	pK_{a2}	pK_{a3}	pK_{a4}	pK_{a5}	pK_{a6}
Catechol	-10 ^a	-1 ^b	-6 ^a	5 ^c	9.45 ^d	12.8 ^d
Methylcatechol	-10 ^a	-1 ^b	-6 ^a	5 ^c	9.6 ^d	12.5 ^d
Dopamine	-10 ^a	-1 ^b	-6 ^a	4.7 ^e	8.9 ^f	13.1 ^g

^a Laviron has determined the pK_{a3} value for hydroquinone to be less than -6 [26]. pK_{a1} is not known but should have a high negative value, thus -10 is used [26]. ^b The pK_{a2} value for duroquinone (-1.1 [29]) has been widely used for other catechols [26-28]. ^c Reference [30]. ^d Reference [31]. ^e Reference [32]. ^f Reference [33]. ^g Reference [34]. The pK_{a1} , pK_{a2} and pK_{a3} values for DHBA, which is structurally very similar with dopamine (Fig. 1), were used here for dopamine [28].

Table 3: Peak potential separation and peak current ratio for 1 mM CA in 0.5 M H₂SO₄ (pH 0.65) and PBS (pH 7.2 and 10.8) at ta-C electrodes.

Scan rate (mV/s)	Cycle #	H ₂ SO ₄ (pH 0.65)		PBS (pH 7.2)		PBS (pH 10.8)	
		ΔE_p (mV)	I_{red} / I_{ox}	ΔE_p (mV)	I_{red} / I_{ox}	ΔE_p (mV)	I_{red} / I_{ox}
10	1 (10)	337 (419)	0.11	388 (740)	0.31	* (*)	*
50	1 (10)	355 (447)	0.53	416 (740)	0.78	145 (*)	0.03
200	1 (10)			549 (725)	0.82	139 (681)	0.09
500	1 (10)	432 (483)	0.51	564 (754)	0.79	168 (674)	0.27
1000	1 (10)			601 (762)	0.79	205 (718)	0.43

*No reduction peak was observed on the CV.

Table 4: Peak potential separation and peak current ratio for 1 mM MC in 0.5 M H₂SO₄ (pH 0.65) and PBS (pH 7.2 and 10.8) at ta-C electrodes. The values at pH 7.2 are the average of two measurements and the standard deviation is within $\pm 10\%$ for the ΔE_p and I_{red}/I_{ox} values.

Scan rate (mV/s)	Cycle #	H ₂ SO ₄ (pH 0.65)		PBS (pH 7.2)		PBS (pH 10.8)	
		ΔE_p (mV)	I_{red}/I_{ox}	ΔE_p (mV)	I_{red}/I_{ox}	ΔE_p (mV)	I_{red}/I_{ox}
10	1 (10)	170 (267)	0.54	307 (629)	0.65	* (*)	
50	1 (10)	249 (330)	0.61	336 (622)	0.80	116 (564)	0.06
200	1 (10)			405 (634)	0.86	142 (580)	0.20
500	1 (10)	293 (330)	0.59	436 (630)	0.87	150 (600)	0.36
1000	1 (10)			545 (685)	0.82	179 (615)	0.53

*No reduction peak was observed on the CV

Table 5: Peak potential separation and peak current ratio for 1 mM DA in 0.5 M H₂SO₄ (pH 0.65) and PBS (pH 7.2) at ta-C electrodes. Data at pH 10.8 is not included because no reduction of dopaminequinone occurred. The values at pH 7.2 are the average of two measurements and the standard deviation is within $\pm 10\%$ for the ΔE_p and I_{red}/I_{ox} values.

Scan rate (mV/s)	Cycle #	H ₂ SO ₄ (pH 0.65)		PBS (pH 7.2)	
		ΔE_p (mV)	I_{red}/I_{ox}	ΔE_p (mV)	I_{red}/I_{ox}
10	1 (10)	240 (320)	0.55	* (*)	
50	1 (10)	284 (357)	0.58	369 (*)	0.11
200	1 (10)			362 (830)	0.53
500	1 (10)	348 (403)	0.57	418 (774)	0.70
1000	1 (10)			442 (727)	0.77

*No reduction peak was seen on the CV

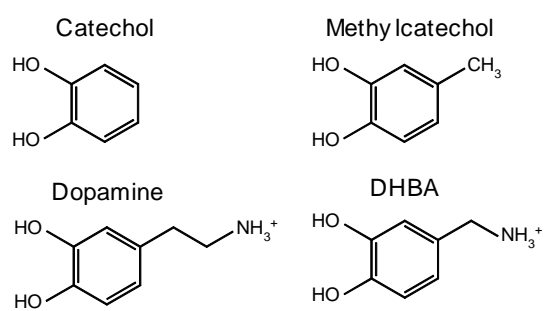
Table 6: Peak potential separation and peak current ratio for 1 mM CA, 1 mM MC and 1 mM DA in PBS (pH 7.2) at GC electrodes.

Scan rate (mV/s)	Cycle #	Catechol		Methylcatechol		Dopamine	
		ΔE_p (mV)	I_{red} / I_{ox}	ΔE_p (mV)	I_{red} / I_{ox}	E_{ox} (mV)	I_{red} / I_{ox}
10	1 (10)	87 (215)	0.83	57 (135)	0.91	61 (*)	0.43
50	1 (10)	92 (206)	0.96	78 (128)	0.98	62 (210)	0.65
200	1 (10)	126 (198)	0.98	116 (148)	0.99	84 (164)	0.83
500	1 (10)	186 (226)	0.97	152 (164)	0.98	114 (134)	0.86
1000	1 (10)	214 (236)	0.97	196 (203)	0.97	142 (160)	0.88

*No reduction peak was observed on the CV

Table 7. Slopes of $\log(I_{ox})$ vs $\log(v)$ and E_{ox} vs pH for catechol, methylcatechol and dopamine.

pH/scan rate	Slope of $\log(I_{ox})$ vs $\log(v)$			Slope of E_{ox} vs pH		
	pH 0.65	pH 7.2	pH 10.8	10 mV/s	50 mV/s	500 mV/s
CA	0.48	0.50	0.29	-0.063	-0.060	-0.059
MC	0.48	0.48	0.38	-0.054	-0.057	-0.055
DA	0.56	0.47	0.38	-0.060	-0.060	-0.060

**Fig. 1**

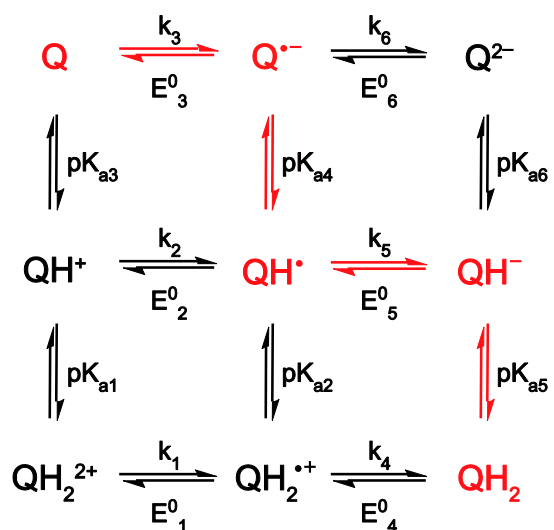


Fig. 2

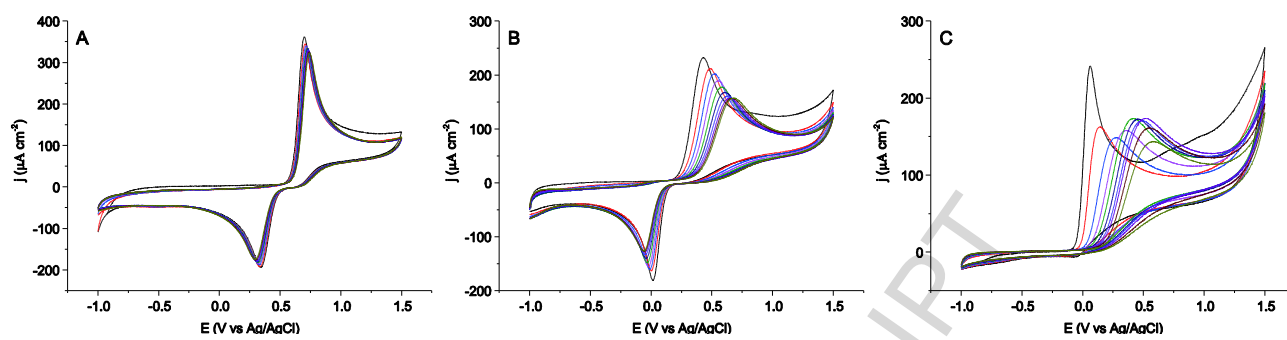


Fig. 3

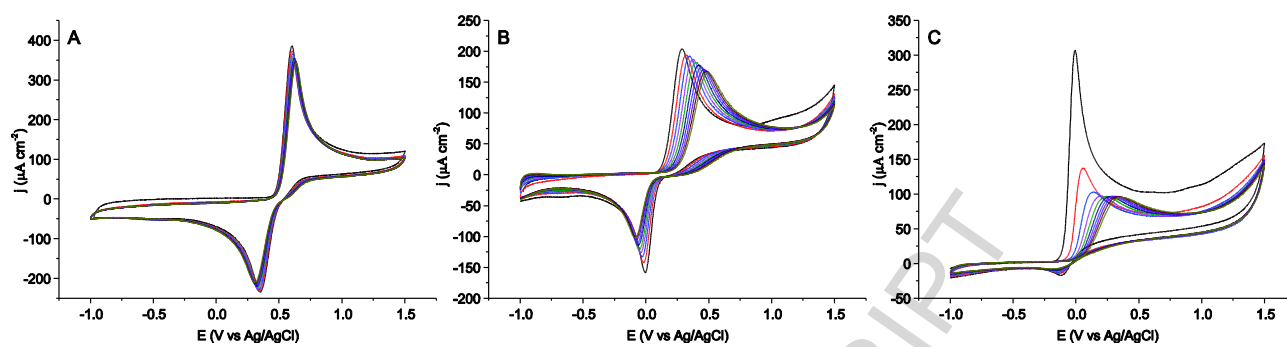


Fig. 4

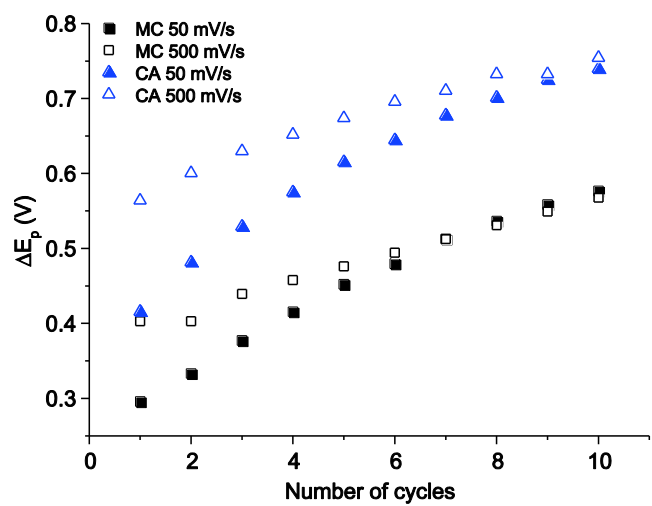


Fig. 5

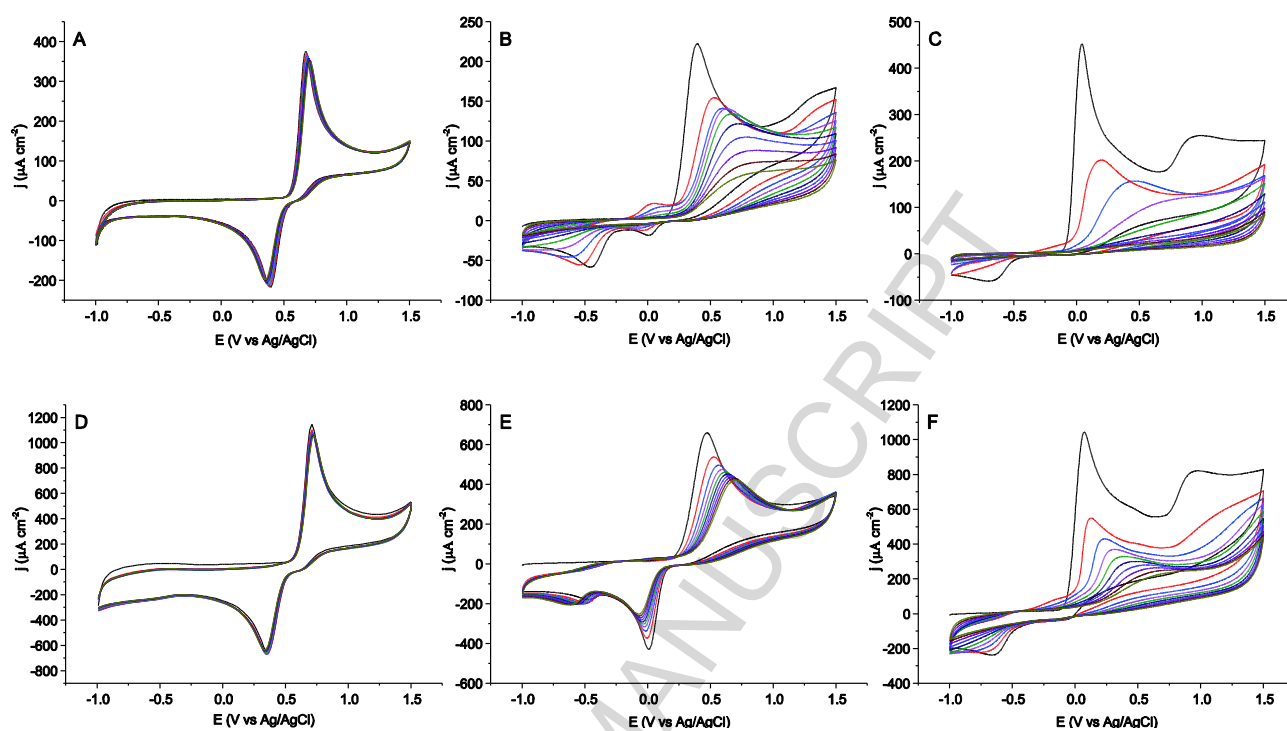


Fig. 6

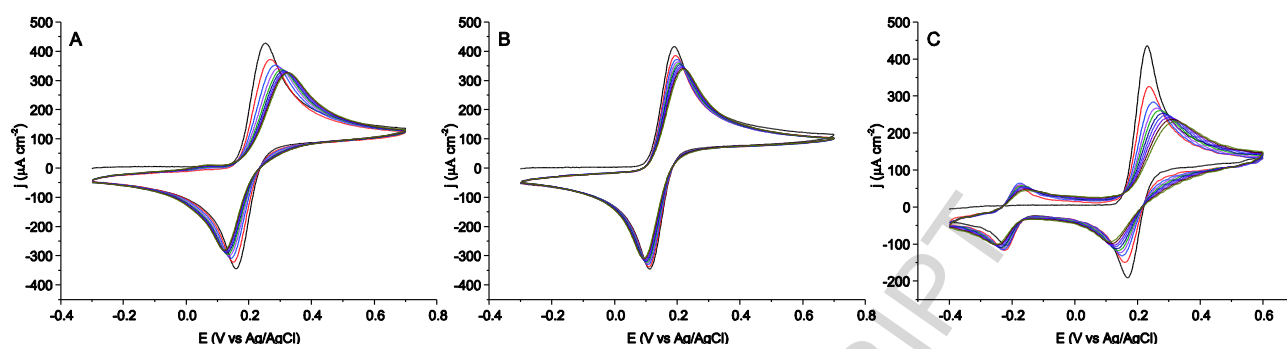


Fig. 7

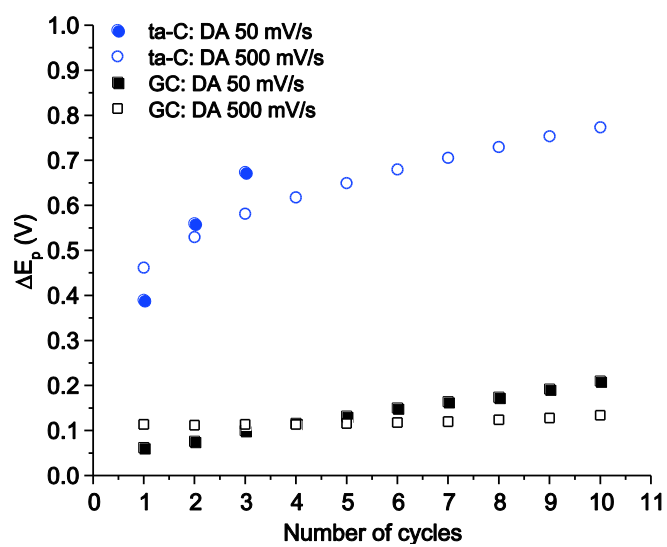


Fig. 8

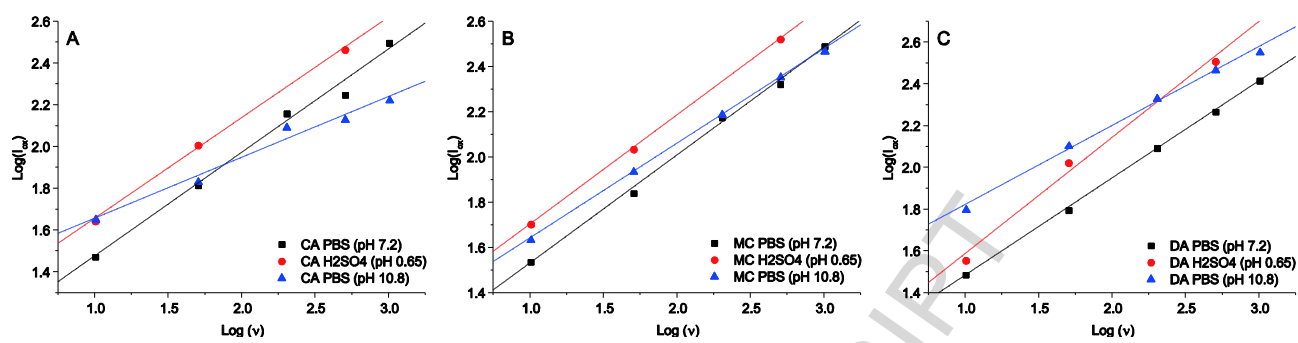


Fig. 9

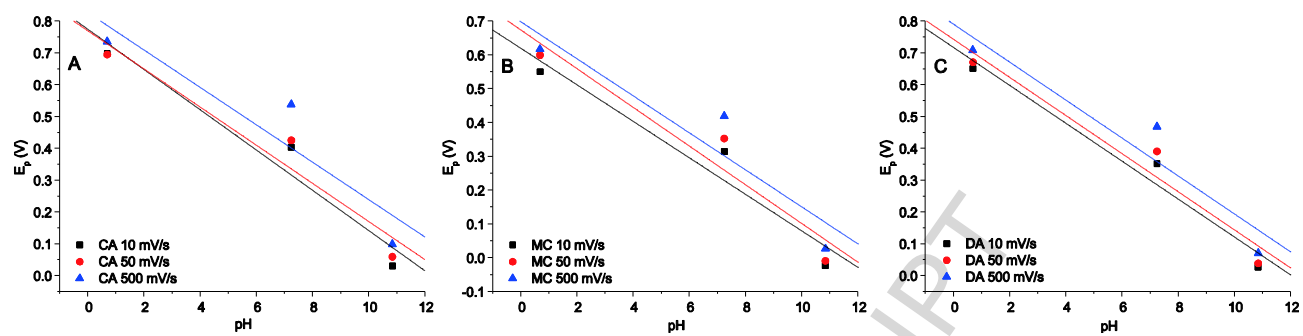


Fig. 10

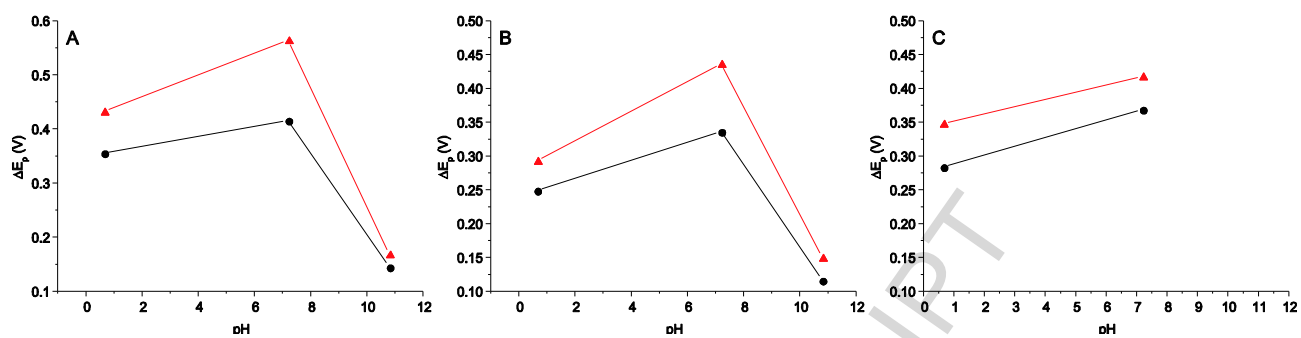


Fig. 11

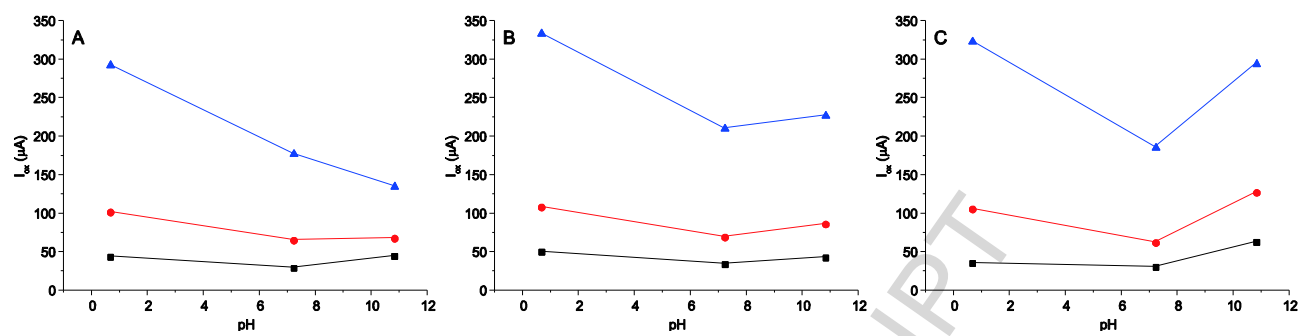


Fig. 12

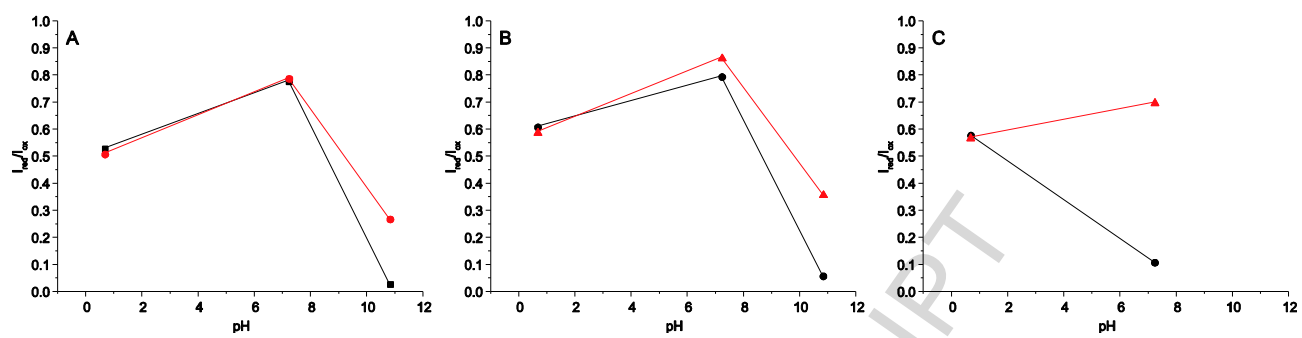
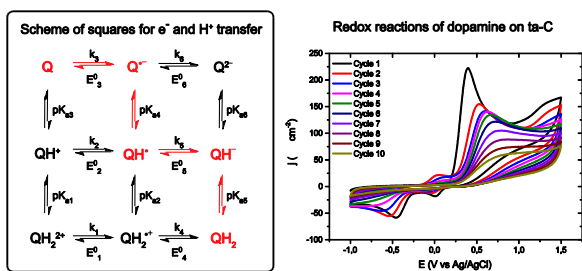


Fig. 13



Graphical abstract

Highlights

- Catechol, methylcatechol and dopamine redox reactions were studied at ta-C electrodes
- All three catechols exhibited sluggish electron transfer kinetics at ta-C
- At neutral and alkaline pH coupled homogeneous reactions followed oxidation
- The coupled reactions led to considerable deterioration of electron transfer kinetics